1 **Sources of non-fossil fuel emissions in carbonaceous aerosols during early winter in Chinese**

2 **cities**

3 Di Liu[1], Jun Li[1*], Zhineng Cheng[1], Guangcai Zhong[1], Sanyuan Zhu[1], Ping Ding[2], Chengde Shen[2],

4 Chongguo Tian[3], Yingjun Chen[4], Guorui Zhi[5], Gan Zhang[1]

6 [1]State Key Laboratory of Organic Geochemistry, Guangzhou Institute of Geochemistry, Chinese

7 Academy of Sciences, Guangzhou, 510640, China

8 [2]State Key Laboratory of Isotope Geochemistry, Guangzhou Institute of Geochemistry, Chinese

9 Academy of Sciences, Guangzhou, 510640, China

10 [3]Key Laboratory of Coastal Environmental Processes and Ecological Remediation, Yantai Institute

11 of Coastal Zone Research, Chinese Academy of Sciences, Yantai 264003, China

12 [4]State Key Laboratory of Pollution Control and Resources Reuse, Key Laboratory of Cities'

13 Mitigation and Adaptation to Climate Change, College of Environmental Science and Engineering,

14 Tongji University, Shanghai 200092, China

15 [5]State Key Laboratory of Environmental Criteria and Risk Assessment, Chinese Research

16 Academy of Environmental Sciences, Beijing 100012, China

17 *To whom correspondence may be addressed:

18 Dr. Jun Li; Email: junli@gig.ac.cn; Tel: +86-20-85291508; Fax: +86-20-85290706

20 **Abstract**

21 China experiences frequent and severe haze outbreaks from the beginning of winter.

22 Carbonaceous aerosols are regarded as an essential factor in controlling the formation and

23 evolution of haze episodes. To elucidate the carbon sources of air pollution, source apportionment

24 was conducted using radiocarbon (^{14}C) and unique molecular organic tracers. Daily 24-hour $PM_{2.5}$

25 samples were collected continuously from October 2013 to November 2013 in 10 Chinese cities.

26 The ^{14}C results indicated that non-fossil fuel (NF) emissions were predominant in total carbon (TC;

27 average = 65 ± 7%). Approximately half of the EC was derived primarily from biomass burning

28 (BB) (average = 46 ± 11%), while over half of the OC fraction comprised NF (average = 68 ± 7%).

29 On average, the largest contributor to TC was NF-derived secondary OC (SOC_{nf}), which

30 accounted for 46 ± 7% of TC, followed by SOC derived from fossil fuels (FF) (SOC_f; 16 ± 3%),

31   BB-derived primary OC (POC_{bb}; 13 ± 5%), POC derived from FF (POC_f; 12 ± 3%), EC derived

32   from FF (EC_f ; 7 ± 2%) and EC derived from BB (EC_{bb}; 6 ± 2%). The regional background

33   carbonaceous aerosol composition was characterized by NF sources; POCs played a major role in

34   northern China, while SOCs contributed more in other regions. However, during haze episodes,

35   there were no dramatic changes in the carbon source or composition in the cities under study, but

36   the contribution of POC from both FF and NF increased significantly.

37

38   **1. Introduction**

39   Recently, a wide range of fine particle ($PM_{2.5}$) pollution has affected northern, central and

40   southern China, particularly on haze days, which has had significant effects on air quality,

41   atmospheric visibility and public health, and caused extensive public and scientific concern (Liu et

42   al., 2013b;Wang et al., 2014). Haze events in Chinese urban areas, especially in megacities, have

43   become a common phenomenon, appearing in every season, because of large and intensive

44   pollutant emissions and unfavorable meteorological conditions (He et al., 2014;Liu et al., 2013c).

45   Generally, heavy and serious haze pollution outbreaks start at the beginning of winter.

46   Carbonaceous aerosols are the important component of $PM_{2.5}$ (~20–80%) (Rogge et al.,

47   1993;He et al., 2004;Dan et al., 2004;Kanakidou et al., 2005) and are regarded as essential for

48   controlling the formation and evolution of haze episodes. Relatively high concentrations of

49   carbonaceous aerosols have been observed during typical haze days in northern, southern and

50   central China (Zhao et al., 2013;Deng et al., 2008;Zhang et al., 2014c). Generally, carbonaceous

51   aerosols (total carbon, TC) can be divided into elemental carbon (EC) and organic carbon (OC)

52   according to their different physical and chemical properties (Krivácsy et al., 2001;Kleefeld et al.,

53   2002). EC is formed either from biomass burning (BB; e.g., wood fires, heating) or fossil fuel

54   combustion (FF; e.g., vehicle or industry emissions such as coal combustion), and can be used as a

55   tracer for primary combustion-generated OC because primary OC and EC are mostly emitted from

56   the same sources (Turpin and Huntzicker, 1995;Strader et al., 1999). OC can be directly derived

57   from primary emissions (primary OC; POC), or formed through oxidation of reactive organic

58   gases followed by gas-to-particle conversion in the atmosphere (secondary OC; SOC) (Choi et al.,

59   2012;Subramanian et al., 2007). Moreover, further subcategories of OC exist, including

60   water-soluble organic carbon (WSOC) and water-insoluble organic carbon (WINSOC), which are

61   distinguished on the basis of water-solubility; these may be essential for assessing the different

62   sources of OC emissions during haze episodes, since WSOC is a proxy for SOC and BB OC,

63   while a large fraction of WINSOC is from POC (Weber et al., 2007b;Docherty et al., 2008;Mayol-

64   Bracero et al., 2002;Weber et al., 2007a;Huang et al., 2014).

65   Several methods have been introduced to identify and quantify OC emission sources, such as

66   the use of organic molecular tracers (Simoneit et al., 1999), receptor models (PMF, CMB)(Singh

67   et al., 2017;Bove et al., 2014;Marcazzan et al., 2003), and dispersion models (Colvile et al., 2003);

68   however, their reliability is limited by their low atmospheric lifetimes, in turn due to chemical

69   reactivity and highly variable emission factors (Fine et al., 2001, 2002, 2004;Gao et al.,

70   2003;Hedberg et al., 2006;Robinson et al., 2006). Recently, radiocarbon (^{14}C) analysis has been

71   used as a powerful tool for facilitating the direct differentiation of non-fossil fuel (NF) carbon

72   sources from fossil fuel (FF) sources, because ^{14}C is completely absent from FF carbon (e.g.,

73   diesel and gasoline exhaust, coal combustion), whereas NF carbon (e.g., biomass burning, cooking

74   and biogenic emissions) shows a high contemporary ^{14}C level (Szidat et al., 2009). Hence, ^{14}C

75   measurements can provide information about the contributions of FF, BB and biogenic emissions

76 to carbonaceous aerosols. Numerous studies have been performed at urban sites and background

77 sites to assess carbonaceous aerosol sources. For example, contemporary carbon was the dominant

78 pollutant in carbonaceous aerosols at a background sites such as Ningbo and Hainan stations (Liu

79 et al., 2013a;Zhang et al., 2014c). In urban, the relative carbon contributions have shown a

80 significant seasonal difference (Yang et al., 2005;Chen et al., 2013;Liu et al., 2013b;Zhang et al.,

81 2014a;Liu et al., 2014a;Zhang et al., 2017). A combination of ^{14}C analysis and organic tracer

82 determination allows for more detailed source apportionment of carbonaceous aerosols (Gelencsér

83 et al., 2007;Ding et al., 2008;Lee et al., 2010;Yttri et al., 2011;Zong et al., 2016;Liu et al.,

84 2015;Zhang et al., 2014b).

85 In this study, sampling was conducted in 10 typical Chinese cities during early winter when

86 heavy haze pollution frequently occurs in this season. Carbonaceous aerosols, including different

87 carbon fractions such as WSOC, WINSOC and EC, along with water-soluble inorganic ions and

88 organic tracers (i.e. anhydrosugars) were analyzed in PM$_{2.5}$ samples. In particular, anhydrosugars

89 such as levoglucosan are used as a molecular marker to indicate biomass-burning emissions. The

90 combination of ^{14}C analysis and the concentration of levoglucosan has offered new insights into

91 the detailed sources of carbonaceous aerosols. So, source apportionment of carbonaceous aerosols

92 was performed using a source apportionment model based on the ^{14}C results and measured

93 chemicals.

94 **2. Materials and Methods**

95 **2.1 Aerosol sampling**

96 Daily 24-hour PM$_{2.5}$ samples were collected continuously on the rooftops of institutes in 10

97 Chinese cities (Figure 1) from October 2013 to November 2013. In total, 292 aerosol samples,

98   including 10 field blanks, were collected on pre-heated (450ºC for 5 h) quartz fiber filters (8 × 10

99   inches; Whatman, UK) using a high volume sampler with a flow rate of 0.3 m^3 min^{-1}. The filters

100   were then wrapped in aluminum foil, packed into air-tight plastic bags, and stored at -20°C in a

101   refrigerator until analysis. $PM_{2.5}$ mass concentrations were determined gravimetrically by state

102   regulatory agencies. All samples were analyzed for OC and EC, and 20 samples, including two

103   filters based on the $PM_{2.5}$ concentrations at each site, were selected for further chemical analysis.

104   Details of the sampling information and meteorological parameters used during sampling are

105   shown in the Supporting Information (SI).

106   **2.2 Chemical analysis**

107   OC and EC were obtained with an off-line carbon analyzer (Sunset Laboratory, Inc., USA) using

108   the thermo-optical transmittance method (NIOSH 870). Water-soluble inorganic ions (Na^+, Cl^-,

109   Ca^{2+}, Mg^{2+}, K^+, NH_4^+, SO_4^{2-} and NO_3^-) were analyzed with an ion chromatographer (83 Basic IC

110   Plus, Metrohm, Switzerland). Anhydrosugars (levoglucosan, galactosan and mannosan) were

111   analyzed by gas chromatography-mass spectroscopy (GC-MS) (7890-5975; Agilent) using a

112   capillary column (DB-5MS; 30m, 0.25 mm, 0.25μm). Analysis methods related to OC and EC,

113   water-soluble inorganic ions (Wang et al., 2012) and anhydrosugars (Liu et al., 2014a;Liu et al.,

114   2014b) were presented elsewhere and a detailed analytical procedure and method are available in

115   the SI.

116   **2.3 Separation of carbon species**

117   A punched section of filtrate was cut and sandwiched in a filtration unit, then extracted with 100

118   mL ultra-pure water (18.2 MΩ). WSOC species were quantified using a total organic carbon (TOC)

119   analyzer (TOC-VCPH; Shimadzu, Japan). The punched filtrate was dried in a desiccator, wrapped

120 in aluminum foil and then stored in a refrigerator. WINSOC and EC were obtained from the

121 water-filtered sample with an off-line carbon analyzer (Sunset Laboratory, Inc.) using the

122 thermo-optical transmittance method (NIOSH 870).

123 **2.4 Radiocarbon measurements**

124 Isolation procedures for the ^{14}C measurements of WSOC, WINSOC and EC have been

125 described previously (Liu et al., 2016b;Liu et al., 2013b). Two filters, based on the $PM_{2.5}$

126 concentrations at each site, were used for ^{14}C determination of WSOC, WINSOC and EC, to

127 distinguish between FF and NF emissions. To obtain the WSOC, WINSOC and EC fractions from

128 a single punch filter, a circular section of the punch filter was clamped in place between a filter

129 support and a funnel and then 60 ml ultra-pure water was slowly passed through the punch filter

130 without a pump, allowing the WSOC to be extracted delicately. WSOC was quantified as the total

131 dissolved organic carbon in solution using a total organic carbon (TOC) analyzer (Shimadzu

132 TOC_VCPH, Japan) following the nonpurgeable organic carbon protocol. WSOC solution was

133 freeze-dried to dryness at -40 °C. The WSOC residue was re-dissolved with ~500 µl of ultra-pure

134 water and then transferred to a pre-combusted quartz tube, which was then placed in the freeze

135 dryer. After that, the quartz tube was combusted at 850 °C. The remaining carbon on the filter was

136 identified as WINSOC or EC by an OC/EC analyzer (Sunset, U.S.). After WSOC pretreatment and

137 freeze-dried, OC is oxidized to CO_2 under a stream of pre-cleaned oxygen pure analytical grade

138 O_2 (99.999%, 30 ml min^{-1}) during the pre-combustion step at 340°C for 15 min. Before the OC is

139 oxidized, the sample is first positioned in the 650 °C oven for about 45 s flash heating. This flash

140 heating has the advantage of minimizing pre-combustion charring, since it reduces pyrolysis of

141 OC. After the OC separation, the filters were removed from the system, placed into a muffle

142 furnace at 375°C, and combusted for 4 h. The filters were then quickly introduced back into the

143 system and oxidized under a stream of pure oxygen at 650°C for 10 min to analyze the EC

144 fraction. Finally, the corresponding evolved CO_2 (WSOC, WINSOC, and EC) was cryo-trapped,

145 quantified manometrically, sealed in a quartz tube and reduced to graphite at 600 °C using zinc

146 with an iron (200 mg, Alfa Aesar, 1.5-3 mm, 99.99%) catalyst for accelerator mass spectrometry

147 (AMS) target preparation. Approximately 200 μg of carbon was prepared for each carbon fraction.

148 All ^{14}C values were reported as the fraction of modern carbon (f_m) after correcting for

149 fractionation with δ^{13}C. The degree of uncertainty in the ^{14}C measurements was in the range of

150 0.2–0.6%. In this study, f_m was converted to the fraction of contemporary carbon (f_c), to eliminate

151 the effects of nuclear bomb tests through application of conversion factors of 1.10 ± 0.05 for EC

152 and 1.06 ± 0.05 for 2013 OC data. Here, the f_m values of OC (OC = WSOC + WINSOC) and TC

153 (TC = WSOC + WINSOC + EC) were calculated by isotopic mass balance. The uncertainties of f_{nf}

154 (and f_m) in WSOC, WINSOC, OC and EC were up to 20%, 20%, 15% and 15%, respectively. The

155 concentration in the field blank was negligible (0.37 ± 0.05 μg cm^{-2}; less than 5% carbon) and no

156 field blank subtraction was made for ^{14}C determination. The system blank F^{14}C was

157 0.0036(SD=0.0001), which translated to a ^{14}C age of around 45,000 years BP.

158 **3. Results and Discussion**

159 **3.1 PM$_{2.5}$, OC and EC concentrations and spatial distribution**

160 PM$_{2.5}$ levels ranged from 21.9 to 482 μg m^{-3}, with an average level of 178 ± 103 μg m^{-3}. A total of

161 98% and 81% of PM$_{2.5}$ exceeded the First Grade National Standard (35 μg m^{-3}) and Second Grade

162 National Standard (75 μg m^{-3}) of China, respectively, indicating relatively poor air quality during

163 sampling days. The OC and EC levels ranged from 0.99 to 75.9 μg m^{-3} (average = 22.8 ± 15.3 μg

164 m^{-3}) and 0.07 to 19.3 μg m^{-3} (average = 3.66 ± 3.28 μg m^{-3}), respectively; thus, OC and EC were

165 major components of PM$_{2.5}$, accounting for 13 ± 8% and 2 ± 1% of PM$_{2.5}$, respectively. The OC

166 and EC levels in this study were generally higher than those recorded previously in more

167 developed cities (e.g., New York, Los Angeles, Erfurt, Kosan) (Kam et al., 2012;Kim et al.,

168 2000;Gnauk et al., 2005;Rattigan et al., 2010), indicating severe carbonaceous pollution and

169 emphasizing the importance of restricting carbonaceous aerosols in China.

170 Northern China has high PM$_{2.5}$ concentrations. As shown in Table 1, the average PM$_{2.5}$

171 concentrations in Beijing (190 ± 79 μg m^{-3}), Xinxiang (245 ± 65 μg m^{-3}), Taiyuan (285 ± 84 μg

172 m^{-3}) and Lanzhou (212 ± 112 μg m^{-3}) were significantly higher than those in central and southern

173 China (from 85 μg m^{-3} in Guangzhou to 123 μg m^{-3} in Wuhan). Shanghai, in the eastern coastal

174 region, had the lowest average PM$_{2.5}$ concentration (67 ± 43 μg m^{-3}). The ratio of total organic

175 matter (TOM; 1.6 × OC + EC) to total fine particle mass ranged from 17.4% to 32.6%, except in

176 Guiyang. Cities in central and southern China, such as Chengdu, Wuhan, Nanjing, and Guangzhou,

177 had a higher ratio of TOM to PM$_{2.5}$ than other cities. Moreover, the OC/EC ratios in those cities

178 were also higher, with values ranging between 8.1 and 12. The spatial distribution pattern closely

179 reflected energy consumption and regional climate differences. In particular, Guiyang, which is a

180 developing city located on the Western plateau, had a high level of PM$_{2.5}$ (227 ± 77 μg m^{-3}),

181 comparable to that in northern China, but also had the lowest levels of OC and EC. Moreover, the

182 TOM to PM$_{2.5}$ ratio was only about 6.0%. This indicates that there are different chemical sources

183 in this developing city compared to megacities in China.

184 **3.2 Radiocarbon results: fraction of modern carbon (f_m)**

185 Table 2 shows the proportion (%) of NF sources in various carbon fractions. Overall, NF

186 emissions represented a more significant proportion of the TC (average = 65 ± 7%; range:

187 50–79%), at all sites, than FF sources, which underscores the importance of NF sources to

188 carbonaceous aerosols during early winter in China.

189 EC is only formed by primary emissions, which are inert in ambient air and originate either

190 from BB or FF combustion. In this study, about half of the EC was derived from BB in the 10

191 urban cities (average 46 ± 11%; range: 24–71%), which represents a slightly higher proportion

192 than that for the same cities in winter and spring, but is similar to previous studies performed in

193 cities in other countries (Szidat et al., 2009;Bernardoni et al., 2013;Liu et al., 2016a). However,

194 this result differs from those obtained in remote regions dominated by BB (Barrett et al.,

195 2015;Zhang et al., 2014a). Compared with other studies in China, the measured biomass burning

196 contributions to EC in Beijing are relatively higher than those in the same city during winter

197 (Zhang et al., 2014b;Zhang et al., 2015b). This is due to the fact that different approach we used

198 for OC/EC separation, and sample selection in this study (selected two filter samples based on

199 relatively lower and higher PM2.5 concentration for each site) because of limitations for ^{14}C

200 analysis (i.e. the bulk samples required and the high cost for ^{14}C measurement). However, the

201 result is similar with those using the same approach (Liu et al., 2016c;Zong et al., 2016). Since

202 limitations for A larger contribution of BB to EC was found in central and western China (i.e.,

203 Beijing, Lanzhou, Chengdu and Guiyang) (49~63%), where Guiyang had the largest proportion of

204 BB in EC (63 ± 12%), followed by Beijing (50 ± 2.0%), Chengdu (50 ± 1.8%), Wuhan (48 ± 10%)

205 and Nanjing (47 ± 5%); this shows that there are large amounts of BB emissions (e.g., from

206 biofuel burning and outdoor fires) in western and central China during early winter. This

207 phenomenon was also found in central China during the severe haze episode that occurred over

China in January 2013, which suggests that these massive BB emissions were generated indoors (i.e., from domestic heating and cooking) and thus could not be detected by MODIS [*Liu et al.*, 2016b]. Guangzhou had the lowest proportion of BB in EC (32 ± 12%), suggesting that FF emissions (coal combustion and vehicle emissions) dominated in the Pearl Delta region. Similar to Guangzhou, Taiyuan and Xinxiang had lower proportions of BB in EC, of 36 ± 11% and 37 ± 1.7%, respectively. High proportions of BB in EC are due to extremely high levels of BB tracers (levoglucosan). In this study, levoglucosan concentrations were in the range 161 to 672 ng m^{-3} (377 ± 153 ng m^{-3}), and were significantly correlated with EC concentrations in BB (r = 0.708, p=0.000).

Over half of the OC fraction was from NF sources at all sites (range: 54–82%), with an average NF source contribution of 68 ± 7%, comparable to previous study reported in four Chinese cities during 2013 winter (Xi'an, Beijing, Shanghai and Guangzhou were 63%, 42%, 51% and 65%, respectively)(Zhang et al. 2015a). Generally, the f_m spatial distribution of OC is similar to that of EC, with NF sources contributing more in central China. Here, OC was divided into WSOC and WINSOC, which has been separated with respect to fossil and NF sources. A large contribution of NF sources to WINSOC (64 ± 7%) was observed in this study, comparable to previous studies performed in urban areas of Europe, e.g., Gothenburg (55 ± 8%) and Zurich (70 ± 7%) (Szidat et al., 2009;Zhang et al., 2013). Moreover, the f_m values for WSOC (70 ± 8%) were slightly higher than those for WINSOC, which showed values comparable to those observed in European and American cities (~70−85%) (Weber et al., 2007a;Szidat et al., 2009;Zhang et al., 2013). A higher f_m value indicated that, for WSOC, the contribution of NF emission sources was greater. WSOC is regarded as a mixture of SOC and BB-derived POC, whereas WINSOC is

230 mainly composed of POC from FF combustion, BB and biogenic sources. In this study, the ratio

231 of WSOC to OC increased significantly with an increase in the proportion of NF sources in OC (r

232 = 0.531, p=0.016); this implies that POC from BB is more water-soluble, or that more NF-derived

233 VOCs were involved in SOC formation.

234 **3.3 Source apportionment of different carbon fractions**

235 A source apportionment model for carbonaceous aerosols, including primary and secondary

236 sources, was applied in this study using measured carbon fractions, anhydrosugars, and ^{14}C

237 isotopic signals. Detailed information on this model has been provided previously (Liu et al.,

238 2014a;Liu et al., 2016a).

239 Briefly, EC from FF combustion (EC$_f$) and BB-derived EC (EC$_{bb}$) can be estimated using the

240 following respective equations:

241 $$EC_f = EC \times (1\text{-}f_c) \qquad\qquad [1]$$

242 $$EC_{bb} = EC \times f_c \qquad\qquad [2]$$

243 Similar to EC, OC can be divided into FF OC (OC$_f$) and NF OC (OC$_{nf}$) based on ^{14}C

244 concentrations. OC$_{nf}$ consists of BB-derived primary OC (POC$_{bb}$), NF-derived SOC (SOC$_{nf}$) and

245 biological primary carbon (BPC), such as spore and plant debris. BPC particles exist mainly in

246 coarse fractions (> 2.5 μm) and only account for ~1% of OC in PM$_{2.5}$ [Guo et al., 2012]. Thus, this

247 carbon fraction was ignored in the present study. POC$_{bb}$ can be semi-quantitatively estimated from

248 Lev concentrations, due to its unique characteristic of originating from BB, as follows:

249 $$POC_{bb} = Lev \times (OC/Lev)_{bb} \qquad\qquad [3]$$

250 According to the levoglucosan/mannosan (Lev/Man; 17.4 ± 5.9) and mannosan/galactosan

251 (Man/Gal; 2.1 ± 0.3) ratios obtained in this study, 7.76 ± 1.47 was adopted as the (OC/Lev)$_{bb}$

252   value [Liu et al., 2014].

253   Thus, the SOC_{nf} fraction can be estimated through subtraction:

254    $$SOC_{nf} = OC_{nf} - POC_{bb} \qquad\qquad [4]$$

255   FF-derived POC and SOC can be estimated by the following respective equations:

256    $$POC_f = WINSOC \times (1\text{-}f_c) \qquad\qquad [5]$$

257    $$SOC_f = WSOC \times (1\text{-}f_c) \qquad\qquad [6]$$

258   Figure 2 shows the proportions of different carbon fractions, including EC_f, EC_{bb}, POC_{bb}, POC_f,

259   SOC_{nf} and SOC_f, in total carbon (TC) for the 10 urban cites during the sampling period. On

260   average, the largest contributor to TC was SOC_{nf}, accounting for $46 \pm 7\%$ of TC, followed by

261   SOC_f ($16 \pm 3\%$), POC_{bb} ($13 \pm 5\%$), POC_f ($12 \pm 3\%$), EC_f ($7 \pm 2\%$) and EC_{bb} ($6 \pm 2\%$). The

262   proportion of primary sources ($POC_{nf} + POC_f + EC_{nf} + EC_f$) (average = $38 \pm 9\%$; range: 25–56%)

263   was lower than that of secondary sources ($SOC_{nf} + SOC_f$) (average = $62 \pm 9\%$; range: 35–83%),

264   which underlines the importance of SOC in carbonaceous pollution.

265   It should be noted that the model uncertainties in these contributions depended mainly on

266   correction factors, such as the $(POC/Lev)_{bb}$ emission ratios for wood burning, and on conversion

267   factors used for determining the f_c in ^{14}C analysis. Typical relative uncertainties were recently

268   estimated, using a similar modelling approach, at 20–25 % for SOC_{nf}, SOC_f, POC_{bb}, and POC_f,

269   and ~13% for EC_f, and EC_{bb} (Zhang et al., 2015a). A large fraction WINSOC can be from

270   secondary organic aerosol as well. Hence POC_f is an upper limit of POC_f. SOC_f may be

271   overestimated if a small fraction (e.g. <20%) WSOC is not secondary, so SOC_f may be an upper

272   limit. Meanwhile, SOC_{nf} may also include other non-fossil sources such as cooking and biogenic

273   emissions, however, they should be limited during wintertime (e.g., <20%). Therefore, our

274   estimates of SOC many generally represent an upper limit but this will not change our conclusion

275   towards to the spatial distribution of SOC in China.

276   POC and EC aerosols are independent from atmospheric gas reaction conditions and thus

277   directly reflect the characteristics of local emission sources. The total proportions of EC_f and POC_f

278   ranged from 10–38%, with an average of 19 ± 9% for all sites. The total proportions of EC_f and

279   POC_f in northern and southern China were greater than in western central and eastern coastal

280   China, indicating a higher impact of FF on local air pollution in both regions. The ratios of POC_f

281   to EC_f (0.66–3.32) were within the emission ratios between coal combustion (2.7–6.1) (Zhang et

282   al., 2008) and traffic exhausts fumes (0.5–1.3) (Zhou et al., 2014;He et al., 2008), indicating that

283   coal combustion and traffic exhaust fumes were the major primary sources at all sites. Beijing (2.6)

284   and Xinxiang (3.3) were mainly dominated by coal combustion emissions. The total proportions

285   of EC_{bb} and POC_{bb} ranged from 12–36%, with an average of 19 ± 8%. West central cities, such as

286   Lanzhou, Chengdu, Guiyang, Nanjing and Wuhan, had large proportions of EC_{bb} and POC_{bb}

287   (average = 23 ± 7%; range: 14–36%), which confirms the greater impact of BB on local air

288   pollution in West central China; this should be considered when setting future limits for polluting

289   corporations.

290   Total SOC in OC ranged from 42–84% (average = 72 ± 10%) among the sites tested in this study,

291   which is similar to recent studies, conducted in the haze period in China of January 2013, which

292   used high-resolution aerosol mass spectrometry; i.e., 41–59% [Sun et al., 2014] and 44–71%

293   [Huang et al., 2014] obtained from online and offline measurements, respectively. There was no

294   significant difference in the SOC/OC ratio among the different regions in China studied herein,

295   except for Guiyang, which had a somewhat lower SOC/OC ratio. Moreover, SOC was comprised

296 predominantly of NF sources at all sites (67–89%), except at Guiyang with values of 42-53%,

297 which are similar to areas in developed countries with good air quality, such as Puy de Dôme,

298 France (86–88%) and Schauinsland, Germany (84–93%) [Gelencsér et al., 2007]. However, our

299 values were higher than those of previous studies conducted in China during other winter and

300 spring seasons, indicating the importance of NF to SOC in China during early winter.

301 **3.4 Comparison of chemicals between samples by PM$_{2.5}$ concentration**

302 Two samples, one each with a low and high PM$_{2.5}$ concentration, were obtained from all 10 study

303 sites (Figure S1) for ^{14}C and inorganic ions analysis, to investigate the composition of

304 carbonaceous aerosols and evaluate the importance of FF and NF carbon in haze formation across

305 China in early winter. During sampling, the air masses generally moved in a northwesterly to

306 northeasterly direction to reach the site. The 5-day back trajectory analysis revealed relatively

307 lower concentrations of PM$_{2.5}$ when the wind speed was higher, and relatively higher PM$_{2.5}$ levels

308 when the wind speed was lower and more stable; synoptic conditions apparently promoted the

309 accumulation of particles (Figure 3).

310 Theoretically, the aerosol composition at higher wind speeds should reflect regional background

311 aerosol characteristics. Figure 3 shows the PM$_{2.5}$ chemical compositions of the stage for lower

312 PM$_{2.5}$ concentration during sampling period. Here, due to the different conversion factors used to

313 transform WINSOC to WINSOM (1.3), and WSOC to WSOM (2.1), OM calculations were based

314 on the relative contributions of WSOC and WINSOC to OC. TOM is the sum of EC, WINSOM

315 and WSOM. Generally, TOM contributions to PM$_{2.5}$ ranged from 21–38%, except in Guiyang

316 where a value of 8% was observed. Moreover, OM was comprised mainly of NF emissions. In

317 cities in northern China (Beijing, Xinxiang and Taiyuan), the contribution of WINSOM (both FF

and NF) was greater, indicating that POC played a major role in regional air quality during this season. Simultaneously, the lower NO_3^-/SO_4^{2-} ratios also implied that POC from FFs might be derived predominantly from coal combustion. The 5-day back trajectory analysis showed that the air mass came from northern China, including regions such as Inner Mongolia and Hebei province, where the ambient temperature is always below 10°C during this season. It is very common for local rural residents to burn coal or biomass fuel to generate heat for their households. Therefore, coal and biomass fuel combustion in northern China might be the major contributor to regional carbonaceous aerosols in northern China during this season. In other cities, WSOM levels in both FF and NF were much higher than those in WINSOM, showing the importance of SOC across China. However, NO_3^-/SO_4^{2-} ratios in Shanghai, Nanjing and Wuhan were much higher than in other areas. The back trajectory results showed that the air mass came from northern China or the Yangtze River Delta, implying that traffic exhaust emissions in those regions was more important for carbonaceous aerosol composition.

The chemical compositions of the higher $PM_{2.5}$ samples obtained in each city are shown in Figure 3. There were no dramatic changes in the carbon source or composition in any of the cities; however, the contribution of EC and WINSOM to both fossil and NF fuels increased significantly, along with the NO_3^-/SO_4^{2-} ratios, indicating the importance of POC from local regions. The back trajectory results showed that wind speeds were moderate and stable, and that synoptic conditions apparently promoted the accumulation of particles derived either from local or regional sources.

4. Conclusion

$PM_{2.5}$ samples were collected continuously from 10 Chinese urban cities during early winter 2013. $PM_{2.5}$, OC and EC levels were highest in northern China, with maximum concentrations of

340 482 μg m^{-3}(Taiyuan, n=31), 75.9 μg m^{-3}(Taiyuan, n=31) and 19.3 μg m^{-3}(Beijing, n=31),

341 respectively. The ^{14}C results, for the lower and higher PM$_{2.5}$ concentration sample pairs obtained

342 in each city, indicated that, overall, NF emissions constituted a significant proportion of TC

343 (average = 65 ± 7%) at all sites, i.e., higher than FF sources. Furthermore, about half of the EC

344 was derived primarily from BB (average = 46 ± 11%), and over half of the OC fraction came from

345 NF sources (average = 68 ± 7%). Source apportionment analysis was done using ^{14}C and unique

346 molecular organic tracers. On average, the largest contributor to TC was SOC$_{nf}$, accounting for 46

347 ± 7% of TC, followed by SOC$_f$ (16 ± 3%), POC$_{bb}$ (13 ± 5%), POC$_f$ (12 ± 3%), EC$_f$ (7 ± 2%) and

348 EC$_{bb}$ (6 ± 2%). When relatively lower PM$_{2.5}$ concentrations were observed, OM was dominant in

349 carbonaceous aerosols, mainly from NF. POC played a major role in regional air quality in the

350 cities in northern China, while SOC contributed more in cities in other regions of China, such as

351 Nanjing and Wuhan. During haze days, there were no dramatic changes in carbon sources or

352 carbon compositions in the sampled cities, but the contributions of POC were relatively higher

353 than the non-haze days.

354

355 **Acknowledgements**

356 This study was supported by the Guangzhou Science and Technology Plan Projects (No.

357 201504010002), the Natural Science Foundation of China (NSFC; Nos. 41430645, 41473101,

358 41503092 and 41373131), and the "Strategic Priority Research Program (B)" of the Chinese

359 Academy of Sciences (Grant No. XDB05040503). All data in this manuscript are freely available

360 on request through the corresponding author (junli@gig.ac.cn). This is a contribution of GIGCAS.

361

362 **Reference**

363 Barrett, T. E., Robinson, E. M., Usenko, S., and Sheesley, R. J.: Source Contributions to Wintertime
364 Elemental and Organic Carbon in the Western Arctic Based on Radiocarbon and Tracer
365 Apportionment, Environmental Science & Technology, 49, 11631-11639, 10.1021/acs.est.5b03081,
366 2015.

367 Bernardoni, V., Calzolai, G., Chiari, M., Fedi, M., Lucarelli, F., Nava, S., Piazzalunga, A., Riccobono, F.,
368 Taccetti, F., Valli, G., and Vecchi, R.: Radiocarbon analysis on organic and elemental carbon in aerosol
369 samples and source apportionment at an urban site in Northern Italy, Journal of Aerosol Science, 56,
370 88-99, http://dx.doi.org/10.1016/j.jaerosci.2012.06.001, 2013.

371 Bove, M. C., Brotto, P., Cassola, F., Cuccia, E., Massabò, D., Mazzino, A., Piazzalunga, A., and Prati, P.:
372 An integrated PM2.5 source apportionment study: Positive Matrix Factorisation vs. the chemical
373 transport model CAMx, Atmospheric Environment, 94, 274-286,
374 http://dx.doi.org/10.1016/j.atmosenv.2014.05.039, 2014.

375 Chen, B., Andersson, A., Lee, M., Kirillova, E. N., Xiao, Q., Kruså, M., Shi, M., Hu, K., Lu, Z., Streets, D. G.,
376 Du, K., and Gustafsson, Ö.: Source Forensics of Black Carbon Aerosols from China, Environmental
377 Science & Technology, 47, 9102-9108, 10.1021/es401599r, 2013.

378 Choi, J.-K., Heo, J.-B., Ban, S.-J., Yi, S.-M., and Zoh, K.-D.: Chemical characteristics of PM2.5 aerosol in
379 Incheon, Korea, Atmospheric Environment, 60, 583-592,
380 http://dx.doi.org/10.1016/j.atmosenv.2012.06.078, 2012.

381 Colvile, R. N., Gómez-Perales, J. E., and Nieuwenhuijsen, M. J.: Use of dispersion modelling to assess
382 road-user exposure to PM2.5 and its source apportionment, Atmospheric Environment, 37,
383 2773-2782, http://dx.doi.org/10.1016/S1352-2310(03)00217-6, 2003.

384 Dan, M., Zhuang, G., Li, X., Tao, H., and Zhuang, Y.: The characteristics of carbonaceous species and
385 their sources in PM2.5 in Beijing, Atmospheric Environment, 38, 3443-3452,
386 http://dx.doi.org/10.1016/j.atmosenv.2004.02.052, 2004.

387 Deng, X., Tie, X., Wu, D., Zhou, X., Bi, X., Tan, H., Li, F., and Jiang, C.: Long-term trend of visibility and
388 its characterizations in the Pearl River Delta (PRD) region, China, Atmospheric Environment, 42,
389 1424-1435, 2008.

390 Ding, X., Zheng, M., Edgerton, E. S., Jansen, J. J., and Wang, X.: Contemporary or Fossil Origin: Split of
391 Estimated Secondary Organic Carbon in the Southeastern United States, Environmental Science &
392 Technology, 42, 9122-9128, 10.1021/es802115t, 2008.

393 Docherty, K. S., Stone, E. A., Ulbrich, I. M., DeCarlo, P. F., Snyder, D. C., Schauer, J. J., Peltier, R. E.,
394 Weber, R. J., Murphy, S. M., Seinfeld, J. H., Grover, B. D., Eatough, D. J., and Jimenez, J. L.:
395 Apportionment of Primary and Secondary Organic Aerosols in Southern California during the 2005
396 Study of Organic Aerosols in Riverside (SOAR-1), Environmental Science & Technology, 42, 7655-7662,
397 10.1021/es8008166, 2008.

398 Fine, P. M., Cass, G. R., and Simoneit, B. R.: Chemical characterization of fine particle emissions from
399 fireplace combustion of woods grown in the northeastern United States, Environmental Science &
400 Technology, 35, 2665-2675, 2001.

401 Fine, P. M., Cass, G. R., and Simoneit, B. R.: Chemical characterization of fine particle emissions from
402 the fireplace combustion of woods grown in the southern United States, Environmental Science &
403 Technology, 36, 1442-1451, 2002.

404 Fine, P. M., Cass, G. R., and Simoneit, B. R.: Chemical characterization of fine particle emissions from

405 the fireplace combustion of wood types grown in the Midwestern and Western United States,
406 Environmental Engineering Science, 21, 387-409, 2004.

407 Gao, S., Hegg, D. A., Hobbs, P. V., Kirchstetter, T. W., Magi, B. I., and Sadilek, M.: Water‑soluble
408 organic components in aerosols associated with savanna fires in southern Africa: Identification,
409 evolution, and distribution, Journal of Geophysical Research: Atmospheres (1984–2012), 108, 2003.

410 Gelencsér, A., May, B., Simpson, D., Sánchez-Ochoa, A., Kasper-Giebl, A., Puxbaum, H., Caseiro, A., Pio,
411 C., and Legrand, M.: Source apportionment of PM2.5 organic aerosol over Europe: Primary/secondary,
412 natural/anthropogenic, and fossil/biogenic origin, Journal of Geophysical Research: Atmospheres, 112,
413 n/a-n/a, 10.1029/2006jd008094, 2007.

414 Gnauk, T., Brüggemann, E., Müller, K., Chemnitzer, R., Rüd, C., Galgon, D., Wiedensohler, A., Acker, K.,
415 Auel, R., Wieprecht, W., Möller, D., Jaeschke, W., and Herrmann, H.: Aerosol characterisation at the
416 FEBUKO upwind station Goldlauter (I): Particle mass, main ionic components, OCEC, and mass closure,
417 Atmospheric Environment, 39, 4209-4218, http://dx.doi.org/10.1016/j.atmosenv.2005.02.007, 2005.

418 He, H., Wang, Y., Ma, Q., Ma, J., Chu, B., Ji, D., Tang, G., Liu, C., Zhang, H., and Hao, J.: Mineral dust
419 and NOx promote the conversion of SO2 to sulfate in heavy pollution days, Scientific reports, 4, 2014.

420 He, L.-Y., Hu, M., Zhang, Y.-H., Huang, X.-F., and Yao, T.-T.: Fine Particle Emissions from On-Road
421 Vehicles in the Zhujiang Tunnel, China, Environmental Science & Technology, 42, 4461-4466,
422 10.1021/es7022658, 2008.

423 He, Z., Kim, Y. J., Ogunjobi, K. O., Kim, J. E., and Ryu, S. Y.: Carbonaceous aerosol characteristics of
424 PM2.5 particles in Northeastern Asia in summer 2002, Atmospheric Environment, 38, 1795-1800,
425 http://dx.doi.org/10.1016/j.atmosenv.2003.12.023, 2004.

426 Hedberg, E., Johansson, C., Johansson, L., Swietlicki, E., and Brorström-Lundén, E.: Is levoglucosan a
427 suitable quantitative tracer for wood burning? Comparison with receptor modeling on trace elements
428 in Lycksele, Sweden, Journal of the Air & Waste Management Association, 56, 1669-1678, 2006.

429 Huang, R.-J., Zhang, Y., Bozzetti, C., Ho, K.-F., Cao, J.-J., Han, Y., Daellenbach, K. R., Slowik, J. G., Platt, S.
430 M., Canonaco, F., Zotter, P., Wolf, R., Pieber, S. M., Bruns, E. A., Crippa, M., Ciarelli, G., Piazzalunga, A.,
431 Schwikowski, M., Abbaszade, G., Schnelle-Kreis, J., Zimmermann, R., An, Z., Szidat, S., Baltensperger,
432 U., Haddad, I. E., and Prévôt, A. S. H.: High secondary aerosol contribution to particulate pollution
433 during haze events in China, Nature, 10.1038/nature13774, 2014.

434 Kam, W., Liacos, J. W., Schauer, J. J., Delfino, R. J., and Sioutas, C.: Size-segregated composition of
435 particulate matter (PM) in major roadways and surface streets, Atmospheric Environment, 55, 90-97,
436 http://dx.doi.org/10.1016/j.atmosenv.2012.03.028, 2012.

437 Kanakidou, M., Seinfeld, J. H., Pandis, S. N., Barnes, I., Dentener, F. J., Facchini, M. C., Van Dingenen,
438 R., Ervens, B., Nenes, A., Nielsen, C. J., Swietlicki, E., Putaud, J. P., Balkanski, Y., Fuzzi, S., Horth, J.,
439 Moortgat, G. K., Winterhalter, R., Myhre, C. E. L., Tsigaridis, K., Vignati, E., Stephanou, E. G., and
440 Wilson, J.: Organic aerosol and global climate modelling: a review, Atmos. Chem. Phys., 5, 1053-1123,
441 10.5194/acp-5-1053-2005, 2005.

442 Kim, Y. P., Moon, K. C., and Hoon Lee, J.: Organic and elemental carbon in fine particles at Kosan,
443 Korea, Atmospheric Environment, 34, 3309-3317, http://dx.doi.org/10.1016/S1352-2310(99)00445-8,
444 2000.

445 Kleefeld, S., Hoffer, A., Krivácsy, Z., and Jennings, S. G.: Importance of organic and black carbon in
446 atmospheric aerosols at Mace Head, on the West Coast of Ireland (53° 19′ N, 9° 54′ W),
447 Atmospheric Environment, 36, 4479-4490, http://dx.doi.org/10.1016/S1352-2310(02)00346-1, 2002.

448 Krivácsy, Z., Hoffer, A., Sárvári, Z., Temesi, D., Baltensperger, U., Nyeki, S., Weingartner, E., Kleefeld, S.,

and Jennings, S. G.: Role of organic and black carbon in the chemical composition of atmospheric aerosol at European background sites, Atmospheric Environment, 35, 6231-6244, http://dx.doi.org/10.1016/S1352-2310(01)00467-8, 2001.

Lee, S., Wang, Y., and Rusell, A. G.: Assessment of secondary organic carbon in the southeastern United States: A review, Journal of the Air & Waste Management Association, 60, 1282-1292, 2010.

Liu, D., Li, J., Zhang, Y., Xu, Y., Liu, X., Ding, P., Shen, C., Chen, Y., Tian, C., and Zhang, G.: The use of levoglucosan and radiocarbon for source apportionment of PM(2.5) carbonaceous aerosols at a background site in East China, Environmental Science & Technology, 47, 10454-10461, 2013a.

Liu, D., Li, J., Zhang, Y. L., Xu, Y., Liu, X., Ding, P., Shen, C. D., Chen, Y. J., Tian, C. G., and Zhang, G.: The Use of Levoglucosan and Radiocarbon for Source Apportionment of PM2.5 Carbonaceous Aerosols at a Background Site in East China, Environmental Science & Technology, 47, 10454-10461, 10.1021/es401250k, 2013b.

Liu, J., Li, J., Zhang, Y., Liu, D., Ding, P., Shen, C., Shen, K., He, Q., Ding, X., Wang, X., Chen, D., Szidat, S., and Zhang, G.: Source Apportionment Using Radiocarbon and Organic Tracers for PM2.5 Carbonaceous Aerosols in Guangzhou, South China: Contrasting Local- and Regional-Scale Haze Events, Environmental Science & Technology, 48, 12002-12011, 10.1021/es503102w, 2014a.

Liu, J., Xu, Y., Li, J., Liu, D., Tian, C., Chaemfa, C., and Zhang, G.: The distribution and origin of PAHs over the Asian marginal seas, the Indian, and the Pacific Oceans: Implications for outflows from Asia and Africa, Journal of Geophysical Research: Atmospheres, 119, 1949-1961, 10.1002/2013jd020361, 2014b.

Liu, J., Li, J., Liu, D., Ding, P., Shen, C., Mo, Y., Wang, X., Luo, C., Cheng, Z., and Szidat, S.: Source apportionment and dynamic changes of carbonaceous aerosols during the haze bloom-decay process in China based on radiocarbon and organic molecular tracers, Atmospheric Chemistry & Physics Discussions, 16, 34949-34979, 2015.

Liu, J., Li, J., Liu, D., Ding, P., Shen, C., Mo, Y., Wang, X., Luo, C., Cheng, Z., Szidat, S., Zhang, Y., Chen, Y., and Zhang, G.: Source apportionment and dynamic changes of carbonaceous aerosols during the haze bloom-decay process in China based on radiocarbon and organic molecular tracers, Atmospheric Chemistry and Physics, 16, 2985-2996, 10.5194/acp-16-2985-2016, 2016a.

Liu, J., Li, J., Liu, D., Ding, P., Shen, C., Mo, Y., Wang, X., Luo, C., Cheng, Z., Szidat, S., Zhang, Y., Chen, Y., and Zhang, G.: Source apportionment and dynamic changes of carbonaceous aerosols during the haze bloom-decay process in China based on radiocarbon and organic molecular tracers, Atmos. Chem. Phys., 16, 2985-2996, 10.5194/acp-16-2985-2016, 2016b.

Liu, J., Mo, Y., Li, J., Liu, D., Shen, C., Ding, P., Jiang, H., Cheng, Z., Zhang, X., Tian, C., Chen, Y., and Zhang, G.: Radiocarbon-derived source apportionment of fine carbonaceous aerosols before, during, and after the 2014 Asia-Pacific Economic Cooperation (APEC) summit in Beijing, China, Journal of Geophysical Research: Atmospheres, 121, 4177-4187, 10.1002/2016jd024865, 2016c.

Liu, X., Li, J., Qu, Y., Han, T., Hou, L., Gu, J., Chen, C., Yang, Y., Liu, X., and Yang, T.: Formation and evolution mechanism of regional haze: a case study in the megacity Beijing, China, Atmospheric Chemistry and Physics, 13, 4501-4514, 2013c.

Marcazzan, G. M., Ceriani, M., Valli, G., and Vecchi, R.: Source apportionment of PM10 and PM2.5 in Milan (Italy) using receptor modelling, Science of The Total Environment, 317, 137-147, http://dx.doi.org/10.1016/S0048-9697(03)00368-1, 2003.

Mayol‑Bracero, O., Guyon, P., Graham, B., Roberts, G., Andreae, M., Decesari, S., Facchini, M., Fuzzi, S., and Artaxo, P.: Water‑soluble organic compounds in biomass burning aerosols over amazonia 2.

Apportionment of the chemical composition and importance of the polyacidic fraction, Journal of Geophysical Research: Atmospheres (1984–2012), 107, LBA 59-51-LBA 59-15, 2002.

Rattigan, O. V., Dirk Felton, H., Bae, M.-S., Schwab, J. J., and Demerjian, K. L.: Multi-year hourly PM2.5 carbon measurements in New York: Diurnal, day of week and seasonal patterns, Atmospheric Environment, 44, 2043-2053, http://dx.doi.org/10.1016/j.atmosenv.2010.01.019, 2010.

Robinson, A. L., Donahue, N. M., and Rogge, W. F.: Photochemical oxidation and changes in molecular composition of organic aerosol in the regional context, Journal of Geophysical Research: Atmospheres (1984–2012), 111, 2006.

Rogge, W. F., Mazurek, M. A., Hildemann, L. M., Cass, G. R., and Simoneit, B. R. T.: Quantification of urban organic aerosols at a molecular level: Identification, abundance and seasonal variation, Atmospheric Environment. Part A. General Topics, 27, 1309-1330, http://dx.doi.org/10.1016/0960-1686(93)90257-Y, 1993.

Simoneit, B. R., Schauer, J. J., Nolte, C., Oros, D. R., Elias, V. O., Fraser, M., Rogge, W., and Cass, G. R.: Levoglucosan, a tracer for cellulose in biomass burning and atmospheric particles, Atmospheric Environment, 33, 173-182, 1999.

Singh, N., Murari, V., Kumar, M., Barman, S. C., and Banerjee, T.: Fine particulates over South Asia: Review and meta-analysis of PM2.5 source apportionment through receptor model, Environmental Pollution, 223, 121-136, https://doi.org/10.1016/j.envpol.2016.12.071, 2017.

Strader, R., Lurmann, F., and Pandis, S. N.: Evaluation of secondary organic aerosol formation in winter, Atmospheric Environment, 33, 4849-4863, http://dx.doi.org/10.1016/S1352-2310(99)00310-6, 1999.

Subramanian, R., Donahue, N. M., Bernardo-Bricker, A., Rogge, W. F., and Robinson, A. L.: Insights into the primary–secondary and regional–local contributions to organic aerosol and PM2.5 mass in Pittsburgh, Pennsylvania, Atmospheric Environment, 41, 7414-7433, http://dx.doi.org/10.1016/j.atmosenv.2007.05.058, 2007.

Szidat, S., Ruff, M., Perron, N., Wacker, L., Synal, H. A., Hallquist, M., Shannigrahi, A. S., Yttri, K. E., Dye, C., and Simpson, D.: Fossil and non-fossil sources of organic carbon (OC) and elemental carbon (EC) in Göteborg, Sweden, Atmos. Chem. Phys., 9, 1521-1535, 10.5194/acp-9-1521-2009, 2009.

Turpin, B. J., and Huntzicker, J. J.: Identification of secondary organic aerosol episodes and quantitation of primary and secondary organic aerosol concentrations during SCAQS, Atmospheric Environment, 29, 3527-3544, http://dx.doi.org/10.1016/1352-2310(94)00276-Q, 1995.

Wang, X., Ding, X., Fu, X., He, Q., Wang, S., Bernard, F., Zhao, X., and Wu, D.: Aerosol scattering coefficients and major chemical compositions of fine particles observed at a rural site in the central Pearl River Delta, South China, Journal of Environmental Sciences, 24, 72-77, http://dx.doi.org/10.1016/S1001-0742(11)60730-4, 2012.

Wang, Y., Wang, M., Zhang, R., Ghan, S. J., Lin, Y., Hu, J., Pan, B., Levy, M., Jiang, J. H., and Molina, M. J.: Assessing the effects of anthropogenic aerosols on Pacific storm track using a multiscale global climate model, Proceedings of the National Academy of Sciences, 111, 6894-6899, 10.1073/pnas.1403364111, 2014.

Weber, R. J., Sullivan, A. P., Peltier, R. E., Russell, A., Yan, B., Zheng, M., De Gouw, J., Warneke, C., Brock, C., and Holloway, J. S.: A study of secondary organic aerosol formation in the anthropogenic‐influenced southeastern United States, Journal of Geophysical Research: Atmospheres (1984–2012), 112, 2007a.

Weber, R. J., Sullivan, A. P., Peltier, R. E., Russell, A., Yan, B., Zheng, M., de Gouw, J., Warneke, C.,

Brock, C., Holloway, J. S., Atlas, E. L., and Edgerton, E.: A study of secondary organic aerosol formation in the anthropogenic-influenced southeastern United States, Journal of Geophysical Research: Atmospheres, 112, n/a-n/a, 10.1029/2007jd008408, 2007b.

Yang, F., He, K., Ye, B., Chen, X., Cha, L., Cadle, S. H., Chan, T., and Mulawa, P. A.: One-year record of organic and elemental carbon in fine particles in downtown Beijing and Shanghai, Atmos. Chem. Phys., 5, 1449-1457, 10.5194/acp-5-1449-2005, 2005.

Yttri, K. E., Simpson, D., Stenström, K., Puxbaum, H., and Svendby, T.: Source apportionment of the carbonaceous aerosol in Norway – quantitative estimates based on 14C, thermal-optical and organic tracer analysis, Atmos. Chem. Phys., 11, 9375-9394, 10.5194/acp-11-9375-2011, 2011.

Zhang, Y.-L., Li, J., Zhang, G., Zotter, P., Huang, R.-J., Tang, J.-H., Wacker, L., Prévôt, A. S. H., and Szidat, S.: Radiocarbon-Based Source Apportionment of Carbonaceous Aerosols at a Regional Background Site on Hainan Island, South China, Environmental Science & Technology, 48, 2651-2659, 10.1021/es4050852, 2014a.

Zhang, Y., Schauer, J. J., Zhang, Y., Zeng, L., Wei, Y., Liu, Y., and Shao, M.: Characteristics of Particulate Carbon Emissions from Real-World Chinese Coal Combustion, Environmental Science & Technology, 42, 5068-5073, 10.1021/es7022576, 2008.

Zhang, Y., Zotter, P., Perron, N., Prévôt, A., Wacker, L., and Szidat, S.: Fossil and non-fossil sources of different carbonaceous fractions in fine and coarse particles by radiocarbon measurement, Radiocarbon, 55, 1510-1520, 2013.

Zhang, Y., Ren, H., Sun, Y., Cao, F., Chang, Y., Liu, S., Lee, X., Agrios, K., Kawamura, K., Liu, D., Ren, L., Du, W., Wang, Z., Prévôt, A. S. H., Szidat, S., and Fu, P.: High Contribution of Nonfossil Sources to Submicrometer Organic Aerosols in Beijing, China, Environmental Science & Technology, 10.1021/acs.est.7b01517, 2017.

Zhang, Y. L., Huang, R. J., El Haddad, I., Ho, K. F., Cao, J. J., Han, Y., Zotter, P., Bozzetti, C., Daellenbach, K. R., and Canonaco, F.: Fossil vs. non-fossil sources of fine carbonaceous aerosols in four Chinese cities during the extreme winter haze episode of 2013, Atmospheric Chemistry & Physics, 15, 1299-1312, 2014b.

Zhang, Y. L., Li, J., Zhang, G., Zotter, P., Huang, R. J., Tang, J. H., Wacker, L., Prévôt, A. S., and Szidat, S.: Radiocarbon-Based Source Apportionment of Carbonaceous Aerosols at a Regional Background Site on Hainan Island, South China, Environmental Science & Technology, 48, 2651-2659, 2014c.

Zhang, Y. L., Huang, R. J., El Haddad, I., Ho, K. F., Cao, J. J., Han, Y., Zotter, P., Bozzetti, C., Daellenbach, K. R., Canonaco, F., Slowik, J. G., Salazar, G., Schwikowski, M., Schnelle-Kreis, J., Abbaszade, G., Zimmermann, R., Baltensperger, U., Prévôt, A. S. H., and Szidat, S.: Fossil vs. non-fossil sources of fine carbonaceous aerosols in four Chinese cities during the extreme winter haze episode of 2013, Atmos. Chem. Phys., 15, 1299-1312, 10.5194/acp-15-1299-2015, 2015a.

Zhang, Y. L., Schnelle-Kreis, J., Abbaszade, G., Zimmermann, R., Zotter, P., Shen, R. R., Schafer, K., Shao, L., Prevot, A. S., and Szidat, S.: Source Apportionment of Elemental Carbon in Beijing, China: Insights from Radiocarbon and Organic Marker Measurements, Environ Sci Technol, 49, 8408-8415, 10.1021/acs.est.5b01944, 2015b.

Zhao, X., Zhao, P., Xu, J., Meng, W., Pu, W., Dong, F., He, D., and Shi, Q.: Analysis of a winter regional haze event and its formation mechanism in the North China Plain, ATMOSPHERIC CHEMISTRY AND PHYSICS, 13, 5685-5696, 2013.

Zhou, R., Wang, S., Shi, C., Wang, W., Zhao, H., Liu, R., Chen, L., and Zhou, B.: Study on the Traffic Air Pollution inside and outside a Road Tunnel in Shanghai, China, Plos One, 9, e112195-e112195, 2014.

581   Zong, Z., Wang, X., Tian, C., Chen, Y., Qu, L., Ji, L., Zhi, G., Li, J., and Zhang, G.: Source apportionment of
582   PM2.5 at a regional background site in North China using PMF linked with radiocarbon analysis:
583   insight into the contribution of biomass burning, Atmospheric Chemistry & Physics, 16, 11249-11265,
584   2016.

585

Table 1 The $PM_{2.5}$, OC and EC data used in this study (average ± standard deviation; $\mu g\ m^{-3}$)

Sites	N	$PM_{2.5}$	OC	EC	OM/$PM_{2.5}$ (%)	OC/EC
Beijing	31	189±79	26.5±12.5	3.6±1.8	24±4.6	7.7±1.8
Xinxiang	31	245±65	29.3±11.7	4.8±2.2	21±4.9	6.5±1.9
Taiyuan	31	285±84	37.3±15.5	7.8±2.8	23±4.4	4.9±1.5
Lanzhou	31	212±112	21.4±9.1	5.0±2.7	19±3.9	4.8±1.2
Guiyang	30	227±77	7.5±4.4	0.76±0.5	6.0±3.4	11±4.4
Chengdu	26	105±39	17.7±8.1	1.8±0.8	28±4.8	10±3.0
Wuhan	22	123±49	17.5±8.3	2.0±1.2	24±8.5	9.6±2.7
Guangzhou	28	85±32	17.4±9.9	2.3±1.8	33±11	8.1±2.4
Nanjing	19	111±50	18.8±8.7	1.6±0.6	28±9.3	12±3.8
Shanghai	27	68±43	7.2±9.0	1.0±0.9	17±8.5	7.4±3.0

Table 2 Proportion of modern carbon in WSOC, WINSOC, OC, EC, TC, and anhydrosugar, and ratio data for 10 urban cites in China for the period October 2013 to November 2013

	Start date	PM$_{2.5}$	WSOC	WINSOC	EC	f$_{m(WSOC)}$	f$_{m(WINSOC)}$	f$_{m(OC)}$	f$_{m(EC)}$	f$_{m(TC)}$	Lev	Lev/OC	Gal	Man
BJ1	11/3/2013	88	5.49	5.62	1.4	0.72	0.73	0.72	0.51	0.70	176	15.9	31.7	65.1
BJ2	11/5/2013	298	23.7	29.2	6.47	0.63	0.67	0.65	0.49	0.63	398	7.50	38.6	79.3
XX1	10/15/2013	132	4,71	17.7	4.30	0.65	0.51	0.54	0.38	0.51	553	24.7	29.3	52.1
XX2	10/22/2013	320	9.29	39.8	6.73	0.64	0.63	0.63	0.35	0.60	601	12.3	31.8	60.8
TY1	10/25/2013	177	15.9	12.5	5.90	0.81	0.66	0.74	0.44	0.69	518	18.2	28.4	56.4
TY2	10/26.2013	314	26.9	26.9	14.2	0.58	0.52	0.55	0.28	0.50	672	12.5	36.3	86.4
LZ1	10/20/2013	123	13.8	2.81	3.74	0.72	0.58	0.70	0.56	0.67	442	26.7	22.6	53.8
LZ2	10/23/2013	199	25.1	7.64	7.51	0.67	0.65	0.66	0.42	0.62	439	13.4	21.4	51.5
GY1	10/31/2013	125	3.74	1.18	0.64	0.57	0.81	0.63	0.71	0.64	247	50.1	16.4	35.5
GY2	11/6/2013	287	9.41	4.36	2.04	0.52	0.78	0.61	0.55	0.60	436	31.7	24.7	64.6
CD1	10/31/2013	53.8	4.40	0.86	0.63	0.87	0.55	0.82	0.51	0.79	198	37.6	13.2	21.2
CD2	11/8/2013	109	14.7	5.59	4.77	0.78	0.71	0.76	0.49	0.71	368	18.2	27.9	46.6
WH1	10/26/2013	73.2	13.0	3.59	1.40	0.69	0.71	0.69	0.42	0.67	344	20.7	15.1	32.0
WH2	10/30/2013	182	25.9	18.1	4.94	0.75	0.73	0.74	0.54	0.72	324	7.37	16.3	30.1
NJ1	10/27/2013	88.2	14.3	2.04	1.48	0.73	0.62	0.72	0.51	0.70	235	14.4	11.9	23.7
NJ2	10/29/2013	149	26.5	7.91	3.42	0.65	0.63	0.64	0.43	0.63	520	15.1	18.6	30.9
GZ1	10/28/2013	67.2	7.40	3.89	2.20	0.79	0.64	0.74	0.41	0.68	161	14.3	10.5	25.3
GZ2	10/29/2013	149	23.1	20.7	5.55	0.69	0.58	0.64	0.24	0.59	279	6.37	13.7	35.6
SH1	10/20/2013	63.2	6.39	1.70	1.58	0.78	0.57	0.73	0.56	0.71	165	20.4	9.77	19.7
SH2	10/23/2013	209	23.8	18.2	5.72	0.75	0.60	0.68	0.33	0.67	468	11.1	18.8	37.2

Note: all fractions are in μg m^{-3}, except for levoglucosan (Lev), galactosan (Gal) and mannosan (Man) (all ng m^{-3}).

586
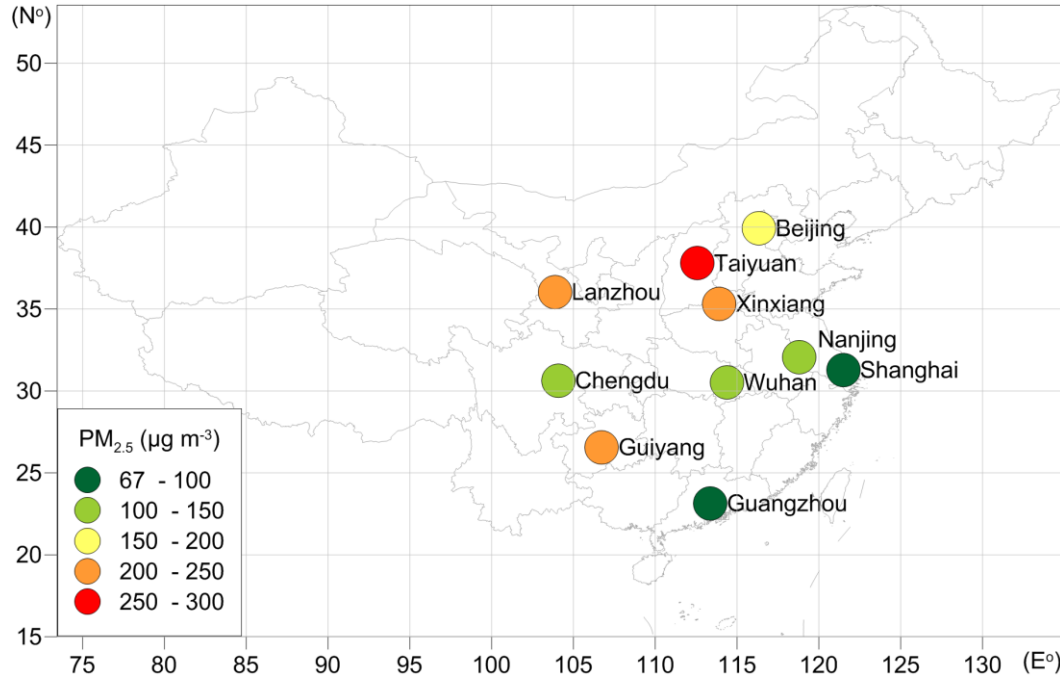
Figure 1. Geographic locations of the 10 Chinese sampling sites. The averages of monitored PM$_{2.5}$

concentrations (daily resolution, n = 31 for each site) during sampling campaign are shown in

color plots.

592
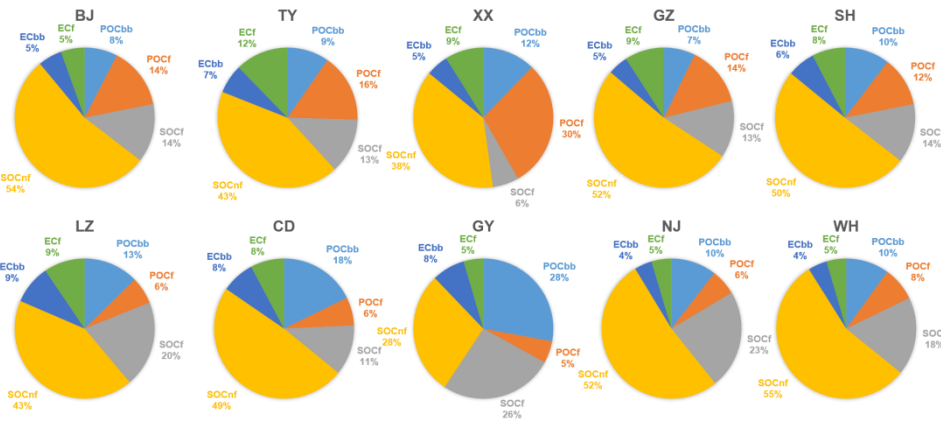
Figure 2. The proportions of different carbon fractions, including elemental carbon derived from

fossil fuels (EC$_f$), EC derived from burning biomass (EC$_{bb}$), BB-derived primary organic carbon

(POC$_{bb}$), POC derived from FF (POC$_f$), non-FF secondary OC (SOC$_{nf}$) and SOC derived from FF

(SOC$_f$) in total carbon (TC) for 10 urban cites during the sampling period.

597

598

599

600

601
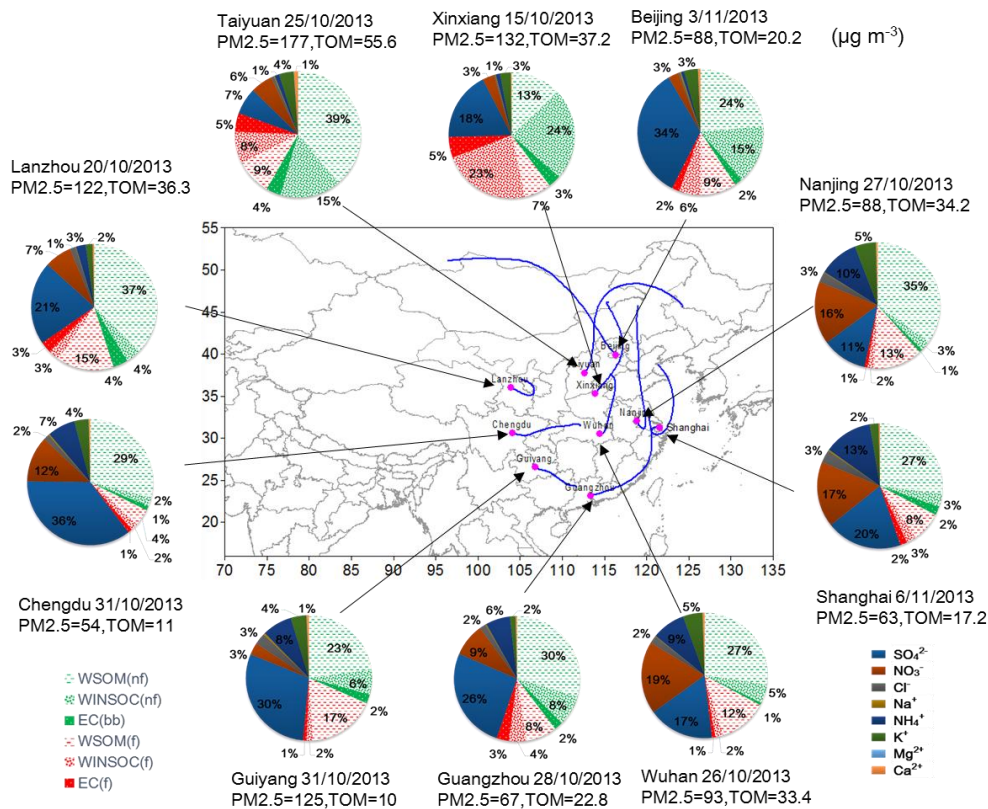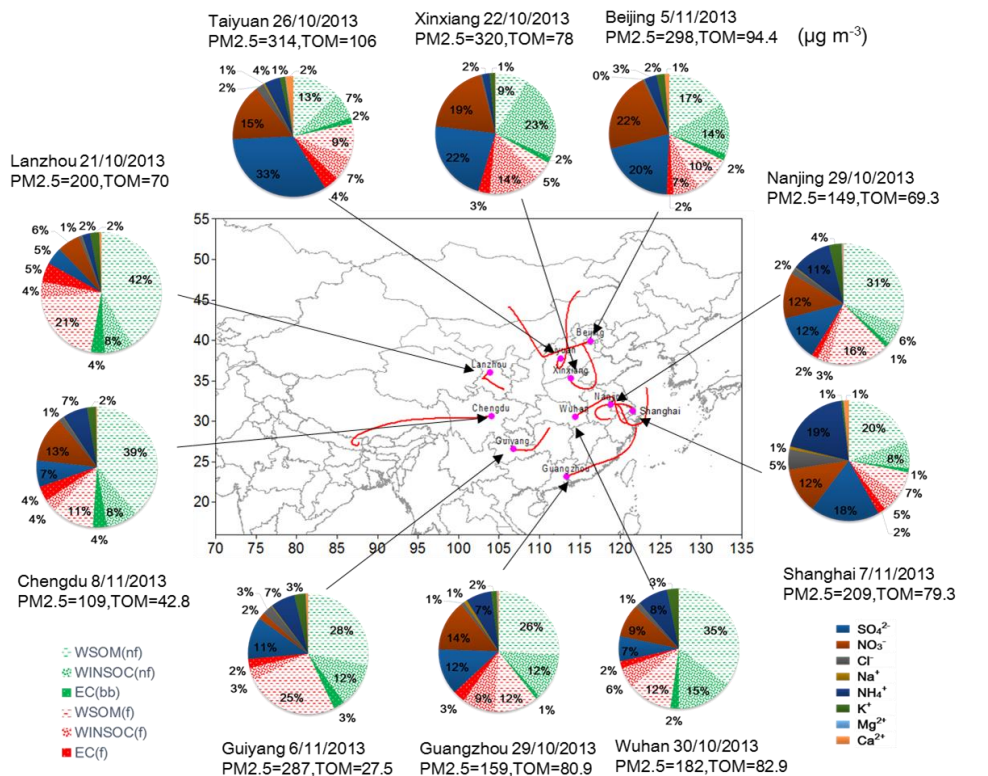
Figure 3. The chemical compositions of fine particles (PM$_{2.5}$) under non-haze (top) and haze

(bottom) conditions during the sampling period.

604

605 The English in this document has been checked by at least two professional editors,

606 both native speakers of English. For a certificate, please see:

607

608 http://www.textcheck.com/certificate/foV8Qb

609